Global Journal of Researches in Engineering: J
General Engineering
Volume 15 Issue 2 Version 1.0 Year 2015
Type: Double Blind Peer Reviewed International Research Journal
Publisher: Global Journals Inc. (USA)
Online ISSN: 2249-4596 Print ISSN:0975-5861

Study of Two-Metal (Cu-Ag) Micro Heat Pipe of Convergent-Divergent Circular Cross Section using different Working Liquids of Low Boiling Point

By KMN S. Iqbal & M. A. R. Akhanda
IUBAT-International University of Business Agriculture and Technology, Bangladesh

Abstract- With the modernization of electronic machines, the size or weight to efficiency ratio is getting small enough to leave the equipment highly thermally stressed. To manage this stress, an experiment on thermal effects of a two-metal (Cu-Ag) micro heat pipe (TMMHP) of convergent-divergent cross section, which provides variable conductivity and pressure gradient, at steady state are investigated to compare with a single metal micro heat pipe (SMMHP). Internal fluid flow is considered as one dimensional which is axially flowing. It is a 150 mm long convergent-divergent hollow circular tube having a hydraulic diameter of 3.74 mm and thickness of 0.3 mm. The evaporator and condenser sections are made of pure copper and silver respectively while the adiabatic section is made of both copper and silver. Water and three low boiling point liquids — ethanol, methanol and iso-propanol — are used as working fluids. In view of the real situation of machines usage, tests are conducted by placing the heat pipe at three different inclinations of 0o, 45o and 90o. To provide heat flux, an electric heater-coil has been wrapped around the evaporator simulating the heat-generation within an actual device, and simultaneously the condenser section is directly cooled by ambient water in an annular space. Ten calibrated K-type thermocouples are installed at different locations — five of them are to measure the temperatures of internal fluid and five are used to measure the surface temperatures of the tube. Temperatures are monitored by digital electronic thermometers. Unlike in the SMMHP, it is found that the super heater effect in the evaporator of TMMHP simplifies the initially developed complex two-phase flow into a single-phase of super heated vapor. Thus, it increases TMMHP's heat transfer capability several times higher than that of a SMMHP.

Keywords: micro heat pipe, two-metal micro heat pipe, TMMHP, convergent-divergent, hydraulic diameter, steady state, one dimensional flow, different inclination.

GJRE-J Classification : FOR Code: 091599

STUDYOFTWOMETALCUAGMICROHEATPIPEOFCONVERGENTDIVERGENTCIRCULARCROSSSECTIONUSINGDIFFERENTWORKINGLIQUIDSOFLOWBOILINGPOINT

Strictly as per the compliance and regulations of :

Study of Two-Metal (Cu-Ag) Micro Heat Pipe of Convergent-Divergent Circular Cross Section using different Working Liquids of Low Boiling Point

KMN S. Iqbal [α] & M. A. R. Akhanda [σ]

Abstract- With the modernization of electronic machines, the size or weight to efficiency ratio is getting small enough to leave the equipment highly thermally stressed. To manage this stress, an experiment on thermal effects of a two-metal (Cu-Ag) micro heat pipe (TMMHP) of convergent-divergent cross section, which provides variable conductivity and pressure gradient, at steady state are investigated to compare with a single metal micro heat pipe (SMMHP). Internal fluid flow is considered as one dimensional which is axially flowing. It is a 150 mm long convergent-divergent hollow circular tube having a hydraulic diameter of 3.74 mm and thickness of 0.3 mm. The evaporator and condenser sections are made of pure copper and silver respectively while the adiabatic section is made of both copper and silver. Water and three low boiling point liquids — ethanol, methanol and iso-propanol — are used as working fluids. In view of the real situation of machines usage, tests are conducted by placing the heat pipe at three different inclinations of 0°, 45° and 90°. To provide heat flux, an electric heater-coil has been wrapped around the evaporator simulating the heat-generation within an actual device, and simultaneously the condenser section is directly cooled by ambient water in an annular space. Ten calibrated K-type thermocouples are installed at different locations — five of them are to measure the temperatures of internal fluid and five are used to measure the surface temperatures of the tube. Temperatures are monitored by digital electronic thermometers. Unlike in the SMMHP, it is found that the super heater effect in the evaporator of TMMHP simplifies the initially developed complex two-phase flow into a single-phase of super heated vapor. Thus, it increases TMMHP's heat transfer capability several times higher than that of a SMMHP.

Keywords: micro heat pipe, two-metal micro heat pipe, TMMHP, convergent-divergent, hydraulic diameter, steady state, one dimensional flow, different inclination.

I. Introduction

Micro heat pipe (MHP) is a heat transferring device based on the phase change phenomenon of fluid contained in it. Before filling with the fluid, the container must be vacuumed to below the atmospheric pressure. MHP is generally of small diameter, usually not over 3.0 mm. The micro heat pipe receives heat at one end to vaporize the fluid which is evaporator, and then travels through the next section losing no heat called adiabatic section, and terminates at the condenser part from where the carried heat dissipates to the atmosphere. Usually, micro heat pipe is made with good heat conducting metal, i.e. copper, stainless steel, nickel etc. Depending on the operating temperature range, selected working fluids may be water or hydrocarbon compounds or it can be cesium, bismuth, sodium, lithium etc. Fluids of low boiling point (LBP) indicate here the fluids that have boiling points below the water at atmospheric pressure. A wick is inserted within the heat pipe spanning end to end to let the condensate crawl back to the evaporator by capillary action. The wick can be made of stainless steel mesh, sintered metal powder, fiber, wire braid etc. In a micro heat pipe, the presence of sharp or non circular edges, and in other cases, radially etched micro grooved inner walls are also replacing wicks to provide the capillary service. Comparing with solid metal, heat transport ability of a heat pipe of the same geometry is found to be many times higher with the same small temperature difference. MHP's applications are widely endorsed in cooling microelectronics and nuclear reactors such as in space satellites. Globally many researchers have been engaged in improving the MHP concepts for the last several decades. A few of their works are cited.

Study on heat pipe has been in practice since 1942 when R. S. Gaugler of General Motors, USA proposed it [1]. However, heat pipes did not receive a target oriented attention until 1963 when Grover et al. [2] directed the heat pipe's condensate-returning mechanism from its confined gravitation-fed state to the simple capillary-force action of wick structure inserted in it. By the U.S. government funding, between 1964 and 1966, RCA was the first corporation to undertake research and development of heat pipes for commercial applications [3]. Starting in the 1980s Sony began incorporating heat pipes into the cooling schemes for some of its commercial electronics products instead of the more traditional finned heat sink with and without forced convection. But, it was twenty years later in 1984 when T. P. Cotter first introduced the idea of "micro" heat pipes [1]. Sreenivasa et al. [4] determined the

Author α σ: IUBAT-International University of Business Agriculture and Technology, 4 Embankment Road Drive, Sector 10, Uttara Model Town, Dhaka 12030. e-mail: kiqbal@iubat.edu

optimum fill ratio in a miniature heat pipe that indicates the same performance as the evaporator section was half filled rather than filling in full. Akhanda et al. [5] tested an air cooled condenser to investigate the thermal performance of MHPs charged with different fluids and oriented a different inclinations. Sakib [6] at Islamic University of Technology (IUT), Organisation of Islamic Cooperation (OIC) has performed tests on different cross sections of MHP of the same hydraulic diameter charged with water at different inclinations. It was found that the best heat transfer coefficient at the circular cross section was at an angle of 90^o vertical. Further observation was made as the thermal resistance of micro heat pipe increases with increasing of flatness ratio and its heat transfer coefficient decreases also with increasing of flatness ratio. Finally, Sakib developed an empirical equation from the experimental data and correlated all his findings which showed $\pm$ 7% nearness with the developed equation. Moon [9] used a miniature heat pipe which was squeezed in the Notebook PC to cool elements that may be heated up to 100^0 C. The output of the experiment using miniature heat pipe with woven wire wicks found it to be a quite viable candidate for a stable cooling unit of Notebook. Babin et al. [10] developed the model that analyzes the heat transport behavior of micro-heat pipe, and presented the model of micro-heat pipe based on the analysis by Chi [11] in a steady-state operation. Longtin et al. [12] presented the improved prediction results, considering partially the shear stress in liquid-vapor interface of groove in a micro heat pipe. Swanson and Peterson [13] analyzed thermo-dynamically the heat transport phenomena in the liquid-vapor interface of heat pipe, and Wu and Peterson [14] studied the thermal performance of micro-heat pipe in an unsteady state. Le Berre et al. [15] studied experimentally the performance of a micro heat pipe array for various filling charges under various experimental conditions. The results showed that the performance of the micro heat pipe array is favored by decreasing the input heat flux or increasing the coolant temperature. Kole and Dey [16] investigated thermal performance using Cu-distilled water nano-fluid, which enhanced thermal conductivity by 15% at 30^oC. Chiang et al. [17] developed a magnetic-nanofluid (MNF) heat pipe (MNFHP) with magnetically enhanced thermal properties. The results showed that an optimal thermal conductivity exists in the applied field of 200 Oe.

Throughout this survey, it has been found that only a single metal or bimetal alloy has been used to manufacture heat pipes including varieties of isometric geometry. In these cases, heat transfer occurs only at constant heat conductivity at both ends of MHP for a single metal or an alloy. No individual or company has attempted doing as investigation on a variable heat conductivity micro heat pipe. Thus, a two-metal micro heat pipe (TMMHP) made with two different metals (i.e. Cu and Ag) of close heat conductivity (i.e. 398 W/m-K for copper and 429 W/m-K for silver) for generating *variable heat conductivity* has been selected by the author Iqbal [8] in his doctoral thesis. Moreover, because of its geometry (convergent-divergent), the pressure gradient of the working fluid will also be variable in the respected TMMHP sub-sections. A series of heat inputs ranging from 2W to 16 W have been supplied to the evaporator keeping the MHP at 0^o to study the heat transfer behavior of pure water along with ethanol, methanol and iso-propanol. Then it was reexamined at 45^o and 90^o positions (evaporator uphill) while the condenser was being cooled by ambient water at a constant flow-rate of 400 ml/min. At the end, the fluid temperatures within the TMMHP as well as the surface temperature at designated locations at steady state have been recorded to compare with other researchers' experimental data. To confirm the reproducibility of the data, the experiments were repeated and found to be the same.

II. Experimental Setup

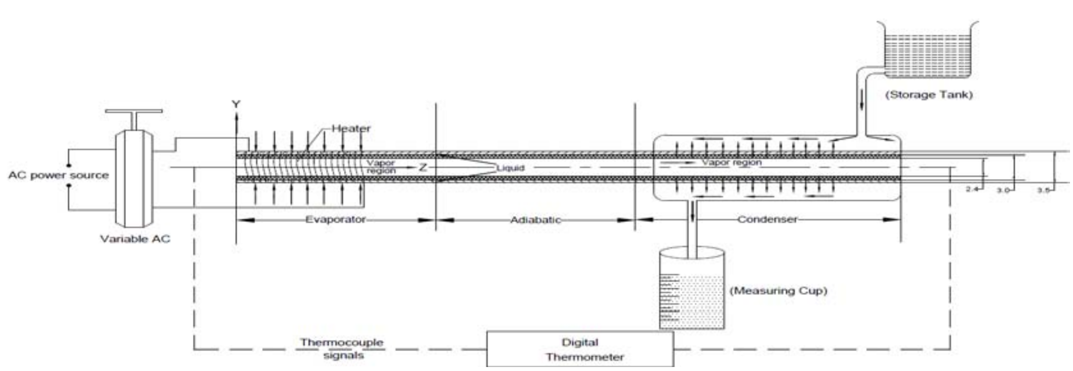

Figure 1 : Schematic diagram of the experimental setup at 0^o inclination

The experimental set up is essentially consisting of a TMMHP, a storage tank, a measuring cup, a power source and a digital thermometer. The schematic diagram of the experimental set up is shown in Figure 1. Table 1 provides the physical dimensions of the TMMHP. The TMMHP used in this experiment is a 150 mm long with a convergent-divergent cross section of 4.5 mm diameter on divergent side and 3.0 mm on convergent made with 0.3 mm thick metal tube which is made half with pure copper and the other half with pure silver. The copper-end is the evaporator section while the silver-end is the condenser. The lengths of the evaporator and adiabatic sections are of equal length of 45 mm each and the rest 60 mm is the condenser section. Thus, the evaporator and condenser are fully covered with copper and silver respectively while the adiabatic section is with both metals. The evaporator side is then welded to seal. For wick, a steel mesh of 0.3 mm thickness with the equal length of TMMHP has been wrapped around a mandrel and inserted into the tube so that the wick radially press fit the inner wall of the tube. Five 1.1 mm holes are drilled according to the Figure 2. Five copper constantan (K-type) thermocouples have been inserted to reach the vapor core and brazed with silver to know the internal working fluid's state. Then another five thermocouples have been attached right beside the holes by quick fixing adhesive to measure the surface temperatures at those locations.

Table 1 : Physical Dimensions of TMMHP (Convergent-Divergent)

Specifications	Dimensions	Materials
Heat pipe total length	150 mm	Copper & Silver
Evaporator section length	45 mm	Copper
Adiabatic section length	45 mm	Copper & Silver
Condenser section length	60 mm	Silver
Divergent side diameter	4.5 mm	
Convergent side diameter	3.0 mm	
Heat pipe profile height	3.8 mm	
Heat pipe wall thickness	0.3mm	
Mesh number of wick	7 holes per cm	
Wick thickness	0.3 mm	
Working liquids	Ethanol, Methanol, Iso-propanol and Water	
No. of surrounding heater in the evaporator section	1 [SGW36]	
Insulating material	(45 + 45) mm	Asbestos rope

The condenser-end of the heat pipe is then plugged into one end of a capillary tube while the other end is attached with a vacuum pump. When pressure within the heat pipe goes well below the atmospheric pressure, then is locked for a couple of minutes to reconfirm its air freeness. Then a pinch-clip is used to choke the capillary tube near the junction, and a slim syringe (Dispovan, 1 ml) filled with 0.60 ml of distilled water, which is 85% (Fill Ratio) of the empty space of the evaporator, is injected into the capillary tube. Actually, the water is sucked into the capillary tube spontaneously because of having lower than atmospheric pressure within the tube. After filling, the condenser-end of the TMMHP is now pinched and sealed by brazing.

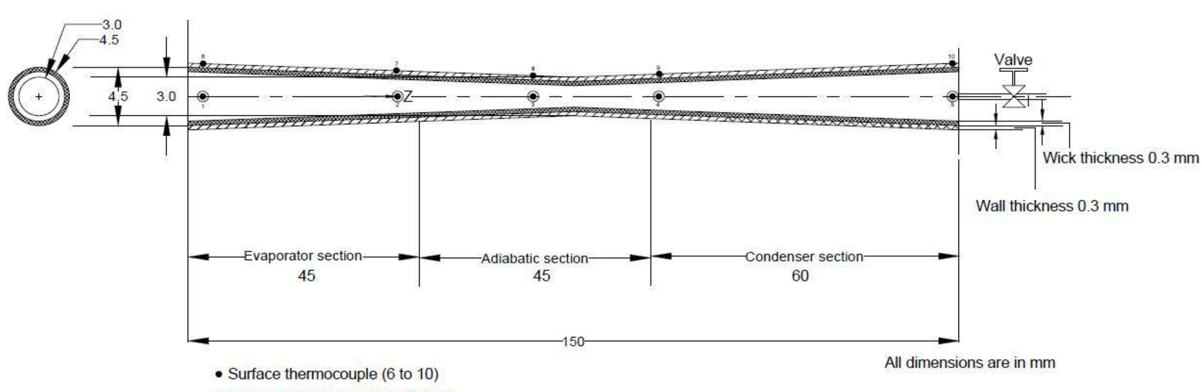

Figure 2 : Positions of thermocouples along the TMMHP

At the evaporator, a fire and electric shock proof tape has been laid around and then SGW36 electric heater wire has been coiled out at a closer pace possible without clinging to each other. To avoid the dispersion of heat produced by the heater in view to keep the heat input value significantly unaltered, the coil was insulated by the asbestos rope by many folds and was extended up to the end of adiabatic section. Finally, another strip of insulating tape was wrapped around to avoid getting soaked by the splash of water. Now the condenser-end of the TMMHP is wrapped up with cotton and inserted into a plastic container which has two outlets. Then the outlets are connected with flexible water tube—upper one is fitted with the valve of the coolant (water) reservoir and the lower one is dipped into an empty bucket to collect the used coolant.

The whole setup is then mounted on a rig which is placed on a wooden table. All the thermocouples have been calibrated and found with ±0.1 degree Celsius variations. Then the thermocouples have been connected with a digital thermometer through a selector switch. The coolant reservoir is filled with the supplied water which is placed above the level of TMMHP. To produce the variable heat input for the heat pipe, a Variac has been introduced, which is then monitored by one ammeter and one precision voltmeter to record the current and voltage simultaneously.

III. Test Procedures

At first the coolant flow is opened to run through the condenser end to ensure the condenser jacket is soaked and fully immersed in water. Then the Variac is connected with the AC power source to produce controlled heat by the heater. The power range is chosen from 2W to 16W producing heat flux ranging 1.9 kW/m^2 to 15.1 kW/m^2 simulating the generated heat in a laptop computer processor and similar electronic equipment [6]. It can be noted, before wrapping the heater coil, its red-hot power limit is checked and found to be 24W. Thus, the upper limit of 16W is quite safe for the experimental purposes. Initially, the TMMHP is inclined at 0° (horizontally), and the time and temperature at the evaporator are recorded until the system reaches steady state. The experiment is continued by keeping the setup at 45° and 90° (vertically) with evaporator uphill position. To attain steady state, a minimum coolant flow rate of 400 ml/min or 70 ml/s has been found to be reasonable to find the used coolant temperature equal to ambient. Although the initial steady-state for 2W is achieved not until ten minutes; however, the subsequent steady-states takes only less than two minutes.

IV. Results and Discussions

Using collected data in this investigation various curves are plotted as shown from Fig. 3 to Fig. 22. Figure 3 shows time required for reaching steady state temperature for different working fluids. It is found that ethanol takes the least time out of four while the other three delayed approximately the same period of time. Methanol and iso-propanol are almost overlapped in terms of temperature rise as well as attaining steady-state condition—this may occur because of their proximity of boiling points (BP). On the other hand, water took longer to reach the BP but at a higher temperature range than the other three. It is observable that although the methanol's boiling is low, still it took the same time period of iso-propanol. This indicates the earlier boiling and condensation of methanol and iso-propanol than other two, which becomes chaotic within the narrow space of the micro heat pipe. Consequently, methanol takes longer period of time to reach thermal equilibrium thus to attend steady state than that of other two hydrocarbons. However, water took the same time but at a higher temperature than the other three because of water's higher latent heat. Therefore, the heat capacity of a fluid not only depends on its thermophysical properties (i.e. density, SG etc.) but also on its chemical bonding (i.e. hydrogen bonding for water).

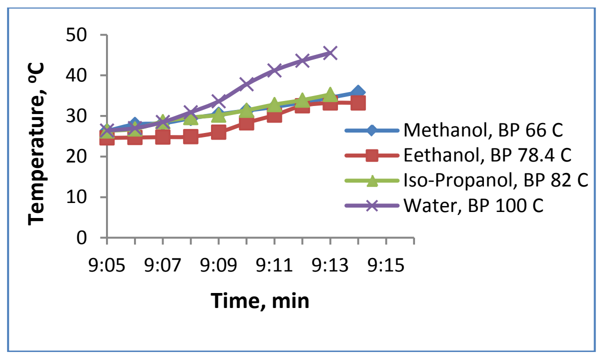

Figure 3 : Time required for reaching steady-state of different fluids

The trends of temperature rises (meter reading minus the ambient, 25°C) at the evaporator section for using different fluids in TMMHP are shown in Figure 4. Other than water, all three are nonlinear. This may happen because of the three are organic compounds and have similar chemical bonding, and the water as an inorganic compound is made up from hydrogen and oxygen's covalent bond. Again it supports the phenomenon that the heat capacity of a fluid is not simply based on thermo physical property (i.e. density, boiling point, SG etc.) rather mainly on its bonding.

V. Evaporator of TMMHP as a Super Heater

Distributions of temperatures along the length of the TMMHP for different working fluids, for different heat inputs, and also for different inclinations are shown from Figure 5 (a) to 12 (b). It is observed from these figures. That in each case of fluid used in TMMHP, there is a temperature rise in the evaporator from T_1 to T_2. Annamalai A. S. *et al.* [7] has reasoned that "In the evaporator zone heat is supplied by an electric coil and the coil surface area density is very high in the middle of the evaporator portion and hence the temperature of the vapor in the middle of the evaporator is high". Authors here disagree with Annamalai that there should be no reason to windup the heater coil densely in the middle of the evaporator rather wrapping must be uniformly done so the produced heat flux remains constant throughout the evaporator. Based on this work and the work of Sakib [6] and Sreenivasa [4], the working liquid should be filled only equal to or less than the empty space (vapor core) of the evaporator of the heat pipe. However, a lot more space in the heat pipe is still vacant to travel during operation. Soon after the MHP goes on operation, boiling starts at the beginning of the heat pipe—part of the fluid evaporates—that leaves a significant room empty within the evaporator which is fully wrapped up by the heater coil. Therefore, when the saturated vapor advances, it continuously receives heat from that part of heater to become superheated, and then it enters the adiabatic section. That's why we notice the temperature rise at point $T_{2,}$ hence this end of the evaporator act as a *super heater*. Regarding the rise of temperature in the evaporator, a comparative relationship between the fluids in the TMMHP and in the SMMHP [6] is shown in Figure 13 (a-c). At the initial steps, the trend for temperature rise for all the fluids are quite similar at 0° inclination; however, they get dispersed at moderately higher heat inputs (i.e. 12W) as the heat pipe is raised to 45° and 90°. This may happen from the "dried out" situation meaning poor capillary pumping of condensate back to the evaporator that leads uniform heating of evaporator. It becomes obvious that the orientation of the TMMHP plays an important role in superheating quality of the fluids. On the other hand, in the case of SMMHP [6, 7] the trend is always negative.

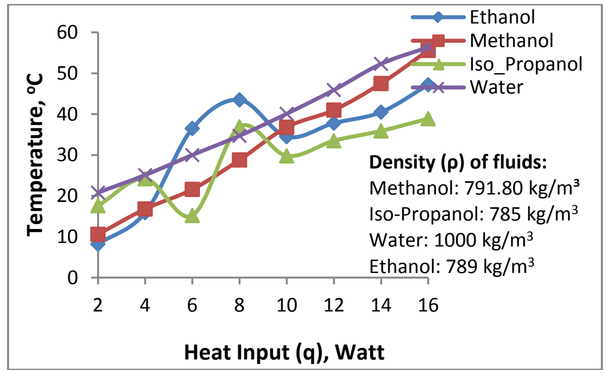

Figure 4 : Rise of fluid temp. vs. heat input at the evaporator

VI. Condenser of TMMHP as an Exothermic Port

It is also noticeable from Figure 5 to Figure 12; there is a rise of temperature of the condensate within the condenser section of the TMMHP. Its convergent-divergent geometry creates a variable pressure gradient throughout the heat pipe that results in a quick pressure drop at the condenser port. Thus the inherent kinetic energy of the condensate increases the terminal temperature which improves the heat transfer of the system. Such an increase of the liquid's temperature also enhances the capillary action which speeds up the rate of evaporation-condensation cycle.

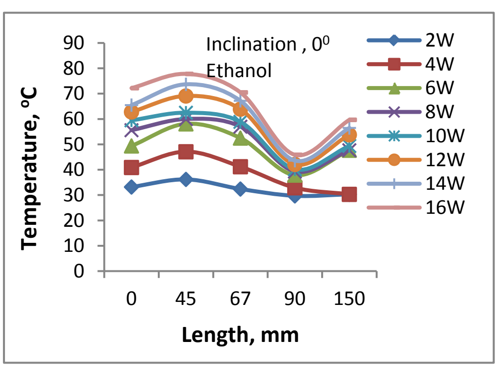

Figure 5 (a) : Fluid temp. distribution along the TMMHP

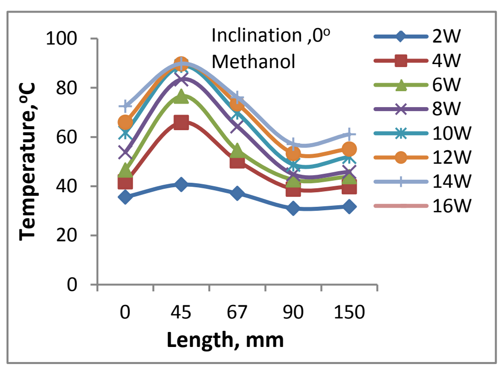

Figure 5 (b) : Fluid temp. distribution along the TMMHP

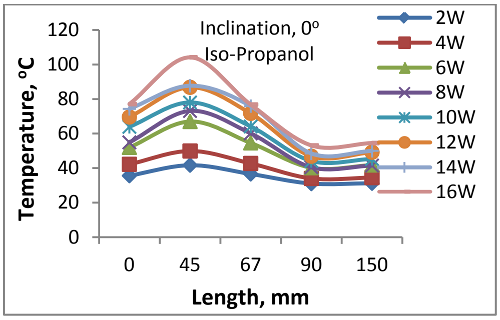

Figure 5 (c) : Fluid temp. distribution along the TMMHP

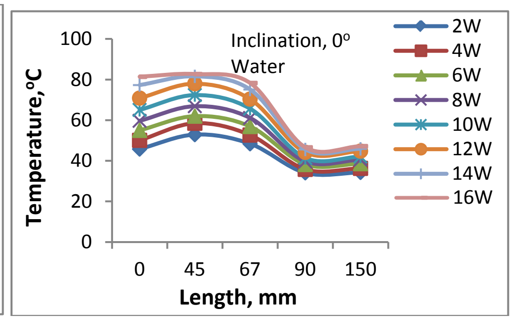

Figure 5 (d) : Fluid temp. distribution along the TMMHP

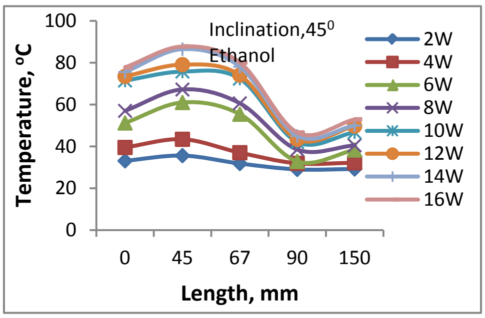

Figure 6 (a) : Fluid temp. distribution along the TMMHP

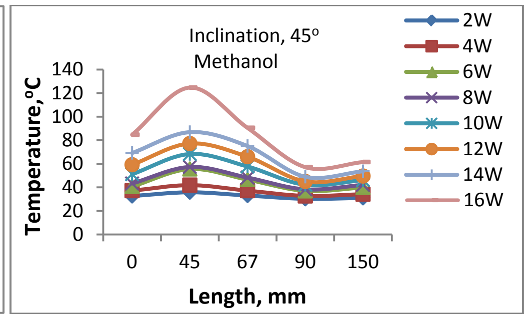

Figure 6 (b) : Fluid temp. distribution along the TMMHP

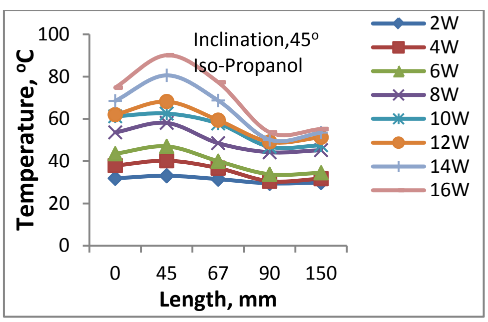

Figure 6 (c) : Fluid temp. distribution along the TMMHP

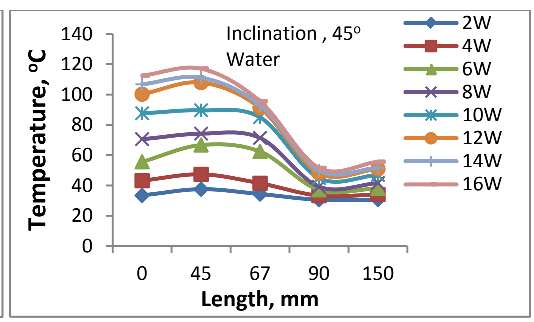

Figure 6 (d) : Fluid temp. distribution along the TMMHP

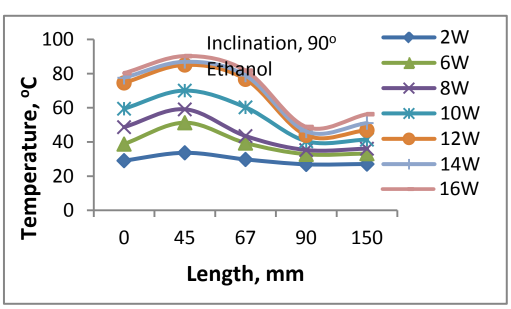

Figure 7 (a) : Fluid temp. distribution along the TMMHP

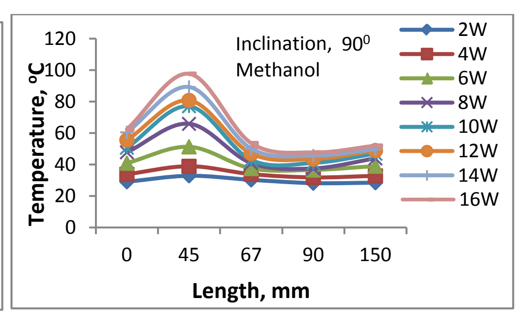

Figure 7 (b) : Fluid temp. distribution along the TMMHP

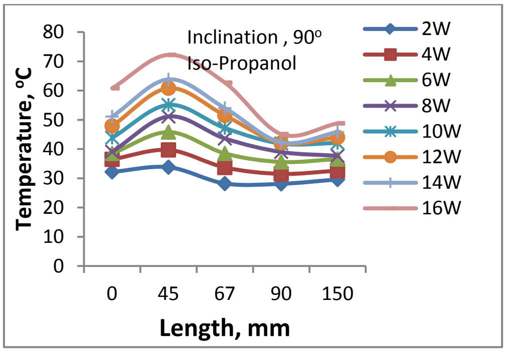

Figure 7 (c) : Fluid temp. distribution along the TMMHP

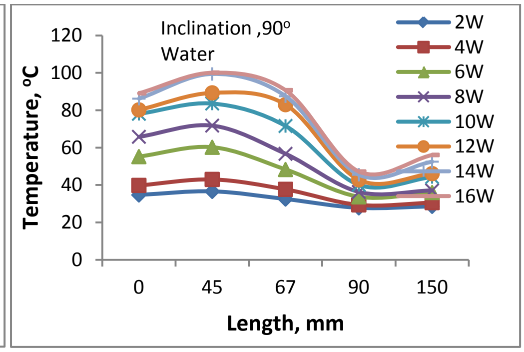

Figure 7 (d) : Fluid temp. distribution along the TMMHP

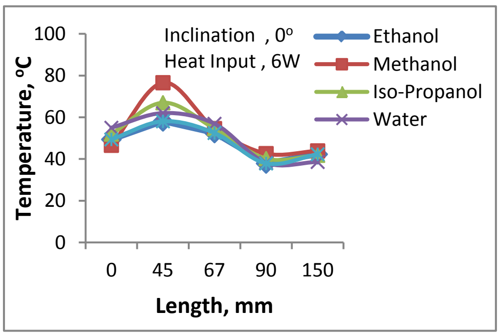

Figure 8 (a) : temp. distribn along the TMMHP

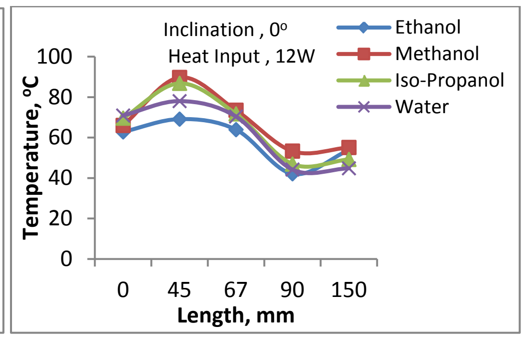

Figure 8 (b) : temp. distribn along the TMMHP

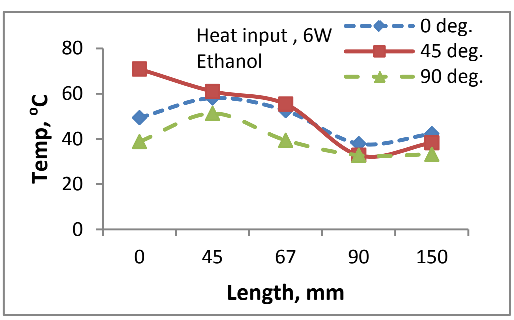

Figure 9 (a) : temp. distribn along the TMMHP

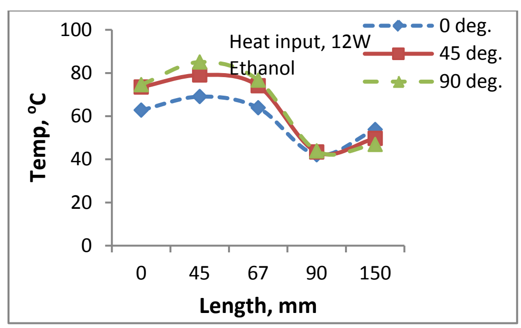

Figure 9 (b) : temp. distribn along the TMMHP

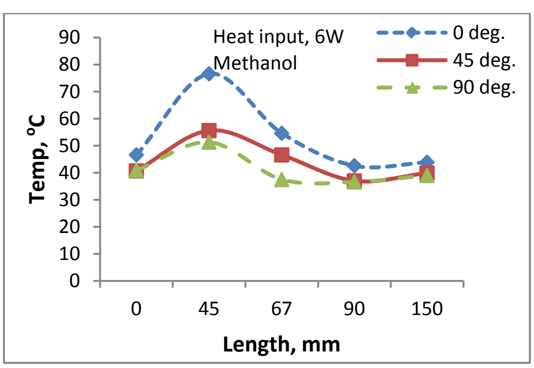

Figure 10 (a) : temp. distribn along the TMMHP

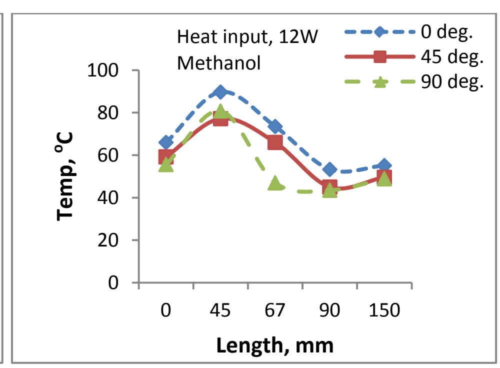

Figure 10 (b) : temp. distribn along the TMMHP

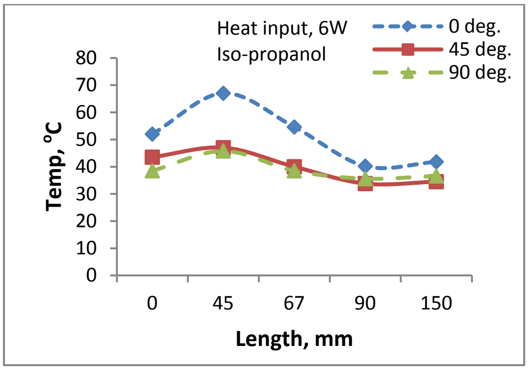

Figure 11 (a) : temp. distribn along the TMMHP

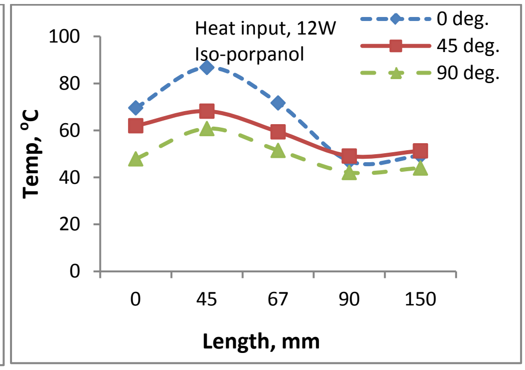

Figure 11 (b) : temp. distribn along the TMMHP

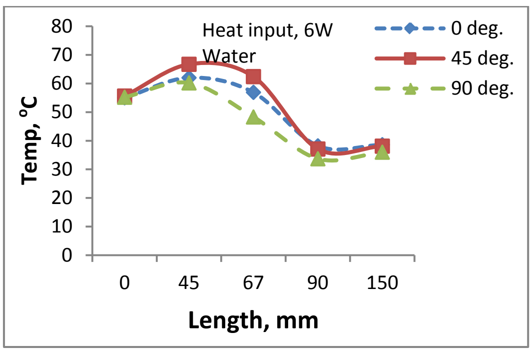

Figure 12 (a) : temp. distribn along the TMMHP

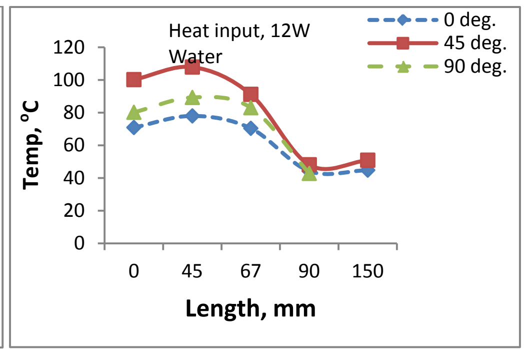

Figure 12 (b) : temp. distribn along the TMMHP

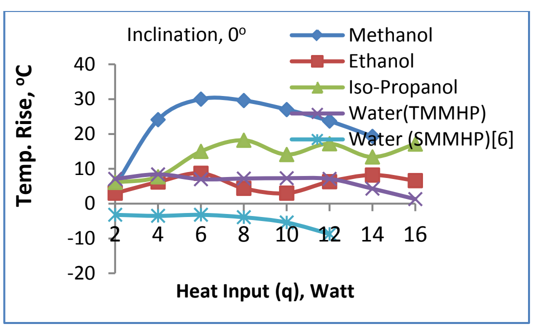

Figure 13 (a)

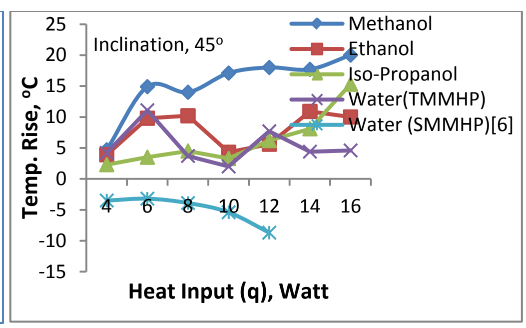

Figure 13 (b)

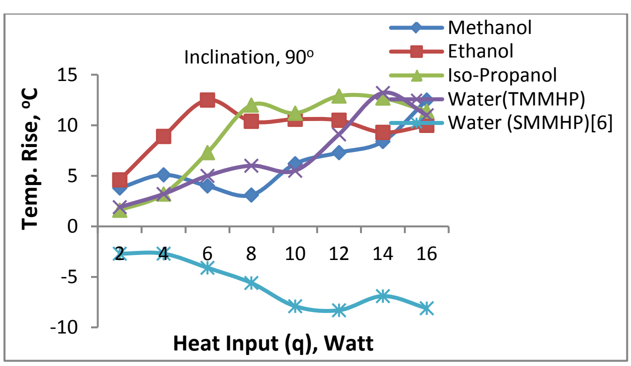

Figure 13 (b)

Figure 13 (a-c) : Comparison of temp. rise (T_2-T_1) of TMMHP with SMMHP [6] of diff. fluids at diff. inclinations

Figure 14 indicates that apparently methanol was condensed within the highest temperature band while water was condensed within the lowest. Such two different temperature bands were identified because of their lower and higher boiling point respectively. On the other hand, the sequence of bandwidth remains increasing for ethanol in all orientations.

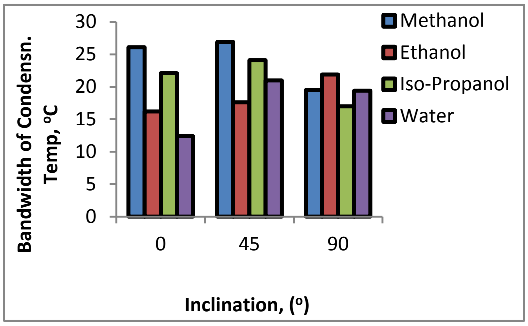

Figure 14 : Band-width of condensn. temp. ($T_{4,16W}$ - $T_{4,2W}$) of diff. fluids for diff. heat inputs applied to TMMHP at diff. inclns

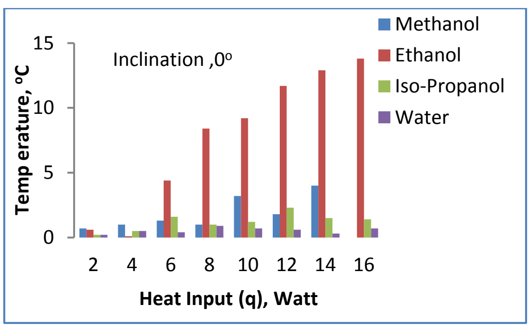

Figure 15 : Comparison of condensn. temp. (T_5-T_4) range of diff. fluids for increasing heat inputs to TMMHP

However, at 90° inclination, the values are scattered because of possible "dried out" situation. Capillary action of the water and hydro-carbons are quite different. As a result, the values of the three hydrocarbons are closely placed while the value of water is a bit apart from them. Thus it is proved again that the heat capacity of a liquid is not only depended on its physical property but also on its chemical property (i.e. structural bonding).

While being condensed, the internal working fluids were experiencing negative temperature gradient within the condenser at circular SMMHP [6], but the convergent-divergent is an exception with a positive gradient as shown in Figure 15. Such negative temperature gradient of fluids is due to continuous heat loss of the saturated liquid throughout the condenser [6]. However, the positive gradient at the convergent-divergent TMMHP is due to sudden pressure drop within its divergent condenser.

During this pressure fall, the inherent kinetic energy of the liquid is converted to heat, hence the temperature of the liquid increases. At the turning point, such a temperature increase of the liquid benefits the capillary action of the wick to drive back condensate even faster to the evaporator. A comparison of thermal performances between the single-metal and two-metal micro heat pipe has been established in the Table 2.

The efficiency of MHP is highlighted by its heat transfer capability at a lower temperature difference. A comparison between the TMMHP and SMMHP [6] is shown in Figure 16. As it is seen, the terminal temperature difference at TMMHP is only the third or even less than that of at SMMHP. This has become possible because of relatively higher conductivity of silver at the condenser port that accelerates the thermodynamic cycle of the working fluid within the heat pipe.

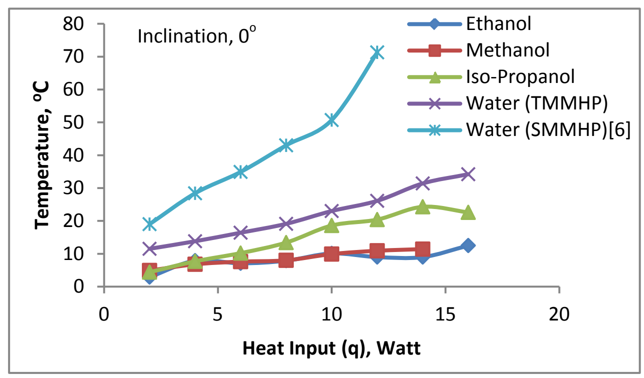

Figure 16 : Comparison of terminal temp. diffs. (T_1-T_5) of TMMHP with SMMHP [6]

a) Comparison of h for water between TMMHP and SMMHP

In Figure 17 and 18, *h* values of water at both SMMHP [6] and TMMHP for different inclinations can be compared. At 0°, the *h* values at TMMHP and SMMHP are almost the same. As the inclination is changed, the *h* values at TMMHP take a new shape which indicates the multiple times higher *h* at lower heat input than that of at SMMHP. However, as the heat input rises the *h* drastically goes down and then become constant. It is noticed, except at horizontal position, the pattern of *h* at both 45° and 90° are the same. If all the operating and test parameters remain the same at both single and two-metal micro heat pipe, then the variability of heat conductivity as well as their operating orientation in TMMHP is considered to be the only initiators for greater value of *h*.

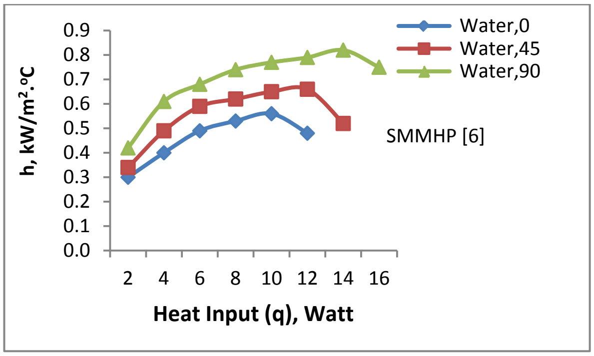

Figure 17 : Convec. HT coeffs. of water in SMMHP [6] at dif. inclns

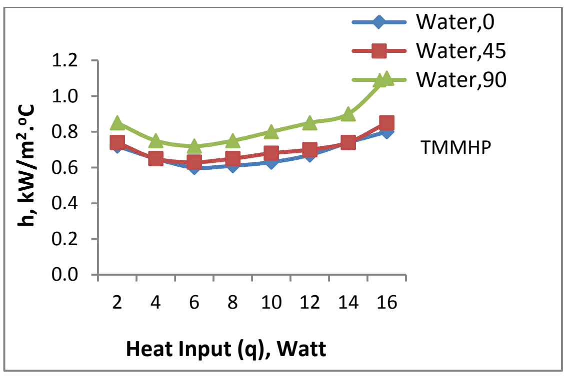

Figure 18 : Convec. HT coeffs. of water at TMMHP at dif. inclns

b) Comparison of h for all fluids between TMMHP and SMMHP

Figure 19 (a-c) shows the values of heat transfer coefficient of different fluids at inclinations of 0^o, 45^o and 90^o. In all orientations, methanol possesses the highest '*h*' among all the fluids, and the highest value is attained at inclination 90^o. Thus in respect to *h*, methanol is the most valuable working liquid out of the four for convergent-divergent TMMHP. Since the surface temperature of the TMMHP is depended on the heat input and heat rejection at the evaporator and condenser respectively, such high values of '*h*' become dependent only on overall thermo physical properties of the internal fluid. However, the sequence of '*h*' values for the four fluids in TMMHP does not keep the same trend as they do in the SMMHP at all three orientations. In Figure 19, the sequential rises of *h* of all four fluids in TMMHP at different angles are shown. In all cases, methanol gains the highest value of *h* whereas the lowest values are not for a particular fluid. According to Newton's law of cooling, *h of a system with constant heat input and surface area gets the highest value for the smallest terminal temperature difference within the heat pipe and vice versa.* This correlation can be authenticated by comparing Figure 16 and Figure 18 where water in TMMHP achieves the highest value of *h*. Consequently, at a small terminal temperature difference, the sharp decrease of pressure gradient leads to rapid condensation at the condenser port to increase the *h* value. The calculated h_{eff} values of all the fluids, based on the average temperature of the evaporator and condenser, for different inclinations are shown in Figure 20. It shows the water and three hydrocarbons are not producing the same pattern of *h* – all are nonlinear. Again it is proved; the value of *h* for any liquid is not only depended on its thermo physical properties but also on its chemical bond.

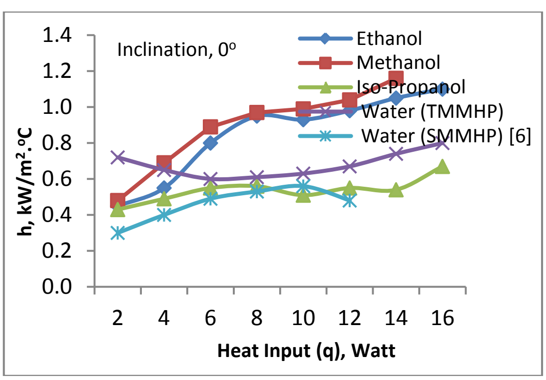

Figure 19 (a) : Convec. coeff. of fluids vs. heat input in TMMHP

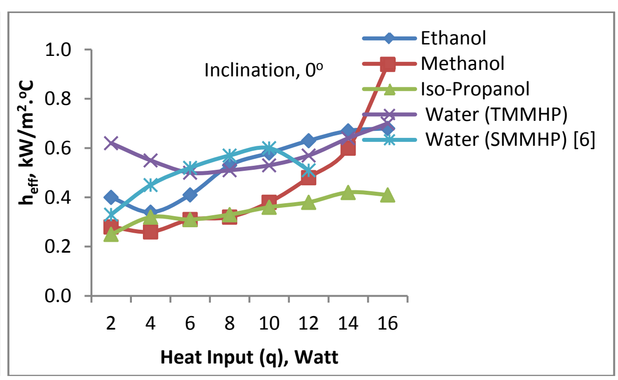

Figure 20 (a) : Eff. convec. coeff. of fluids vs. heat input in TMMHP

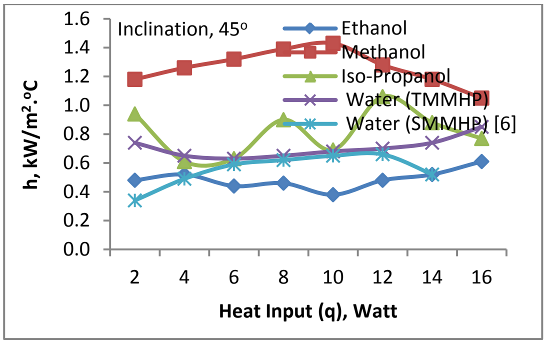

Figure 19 (b) : Convec. coeff. of fluids vs. heat input in TMMHP

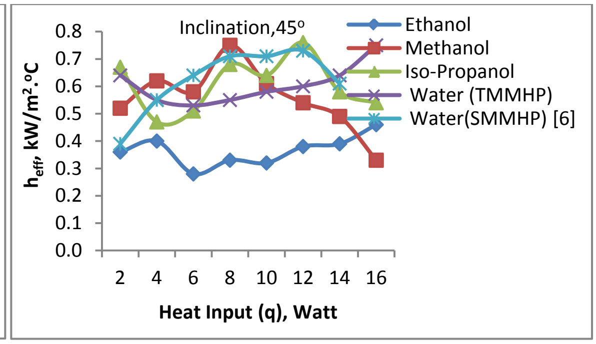

Figure 20 (b) : Eff. convec. coeff. of fluids vs. heat input in TMMHP

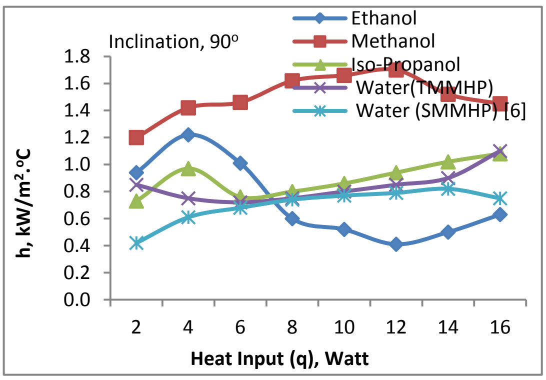

Figure 19 (c) : Convec. coeff. of fluids vs. heat input in TMMHP

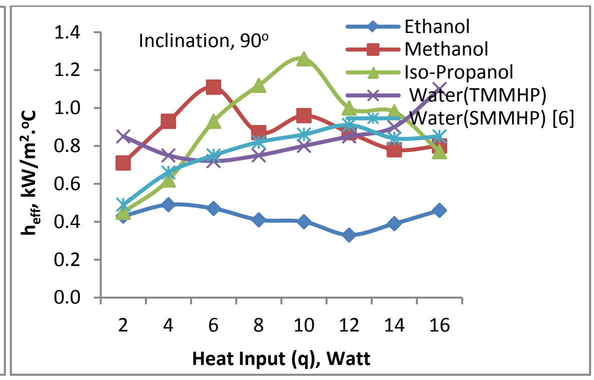

Figure 20 (c) : Eff. convec. coeff. of fluids vs. heat input in TMMHP

Density is a thermo physical property of a fluid. Therefore, when the vapor becomes liquid at the condenser; the density of the fluid therein goes many folds high. Nevertheless, *h* keeps no direct relationship with the density alone which reflects in both Figure 19 and Figure 20. Rather it is found that *h is compositely related with the fluid's density, pressure drop and heat input.* This relationship can be expressed by $h = f(\rho(p(q)))$. Then the authors have developed the dimensionless correlations from this relationship presented later. In Figure 21(a-b), all the fluids' dimensionless heat transfer coefficients are shown including the water's h/h_{eff} at SMMHP [6]. The maximum value of methanol is seen both at 0° and 45° which is quite in match with its *h* value (Fig.19 a-b). However, a little deviation at 90° for methanol indicates the experimental error that spikes up the value of iso-propanol.

However, comparing the water's h/h_{eff} value at TMMHP is higher than that of at SMMHP [6]. Thus, the two different thermal conductivities at the two ports of the TMMHP initiate the quicker heat removal than it does in the SMMHP, hence improves the *h* so greatly.

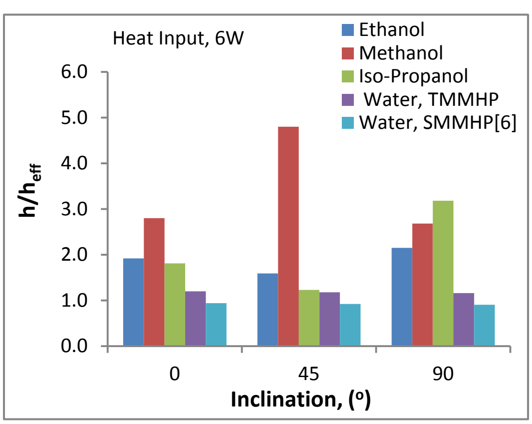

Figure 21(a) : Comparison of h/hef between TMMHP and SMMHP [6]

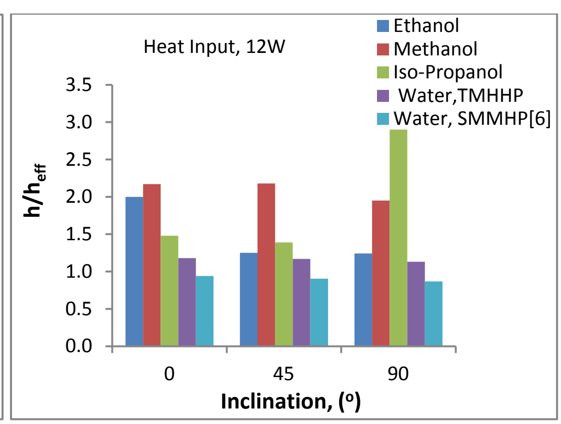

Figure 21(b) : Comparison of h/hef between TMMHP and SMMHP [6]

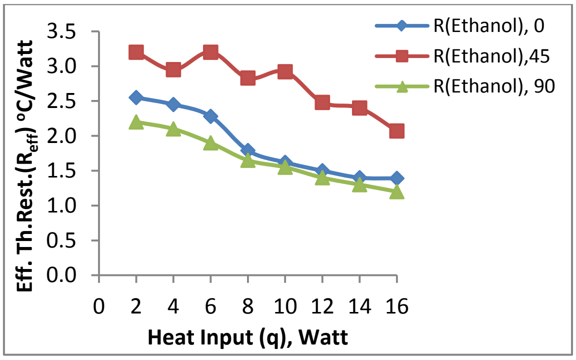

Figure 22 (a) : Thermal Resistance Vs. Heat input at TMMHP

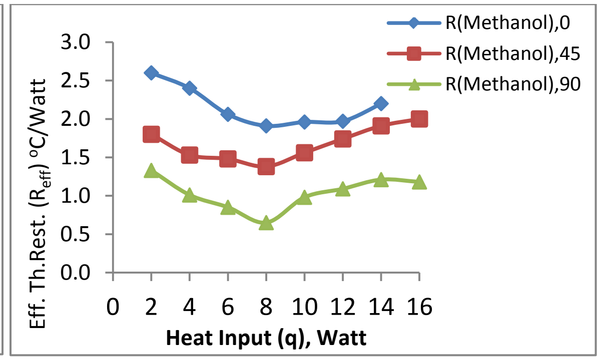

Figure 22 (b) : Thermal Resistance Vs. Heat input at TMMHP

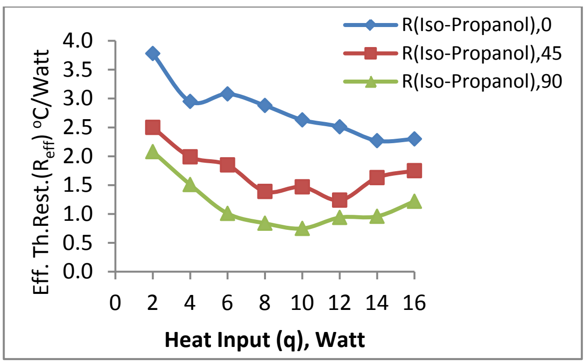

Figure 22 (a) : Thermal Resistance Vs. Heat input at TMMHP

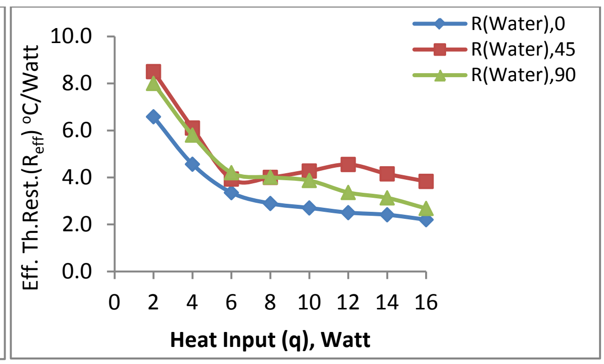

Figure 22 (b) : Thermal Resistance Vs. Heat input at TMMHP

In Figure 22(a-d), the effect of thermal resistances for all four fluids is shown. Except water, the rest three fluids keep almost the same pattern of resistance in the convergent-divergent TMMHP with respect to heat input. Again, the reason can be the difference of their chemical bonding—water is covalent compound and the other three are hydrocarbons. However, a variation of resistance in different fluids is obvious according to the inclination of the experimental setup. Another obvious thing is seen, as the heat input increases to the moderately higher value (i.e. 10W) the resistance goes higher in all four cases and in all inclinations. Since all other parameters are fixed, the geometry of the micro heat pipe is causing this upper trend. Still there are some irregularities between the heat input intervals; those are because of "dry out" situation in the evaporator. As it is noticed, the time required for evaporation-condensation is very low in the convergent-divergent TMMHP; the capillary pumping of the wick is not enough to reach the evaporator. In case of water, by comparing Figure 18 for h and Figure 22(c) for R_{eff}, it is seen the trend of the curves is almost alike. In respect to the heat input, it can be deduced that such decreasing-increasing path is maintained by the internal variability of the conductivity of the two different metals (Cu-Ag). In addition, the convergent-divergent geometry of the TMMHP which also guides the variability of pressure that induces variation of heat transfer. However, methanol poses the lowest thermal resistance 0.65 °C/Watt out of four fluids used in this study.

A comparison of thermal performance between single-metal (SMMHP) [6] and two-metal micro heat pipe (TMMHP) observed in this study is given in Table 2.

Table 2 : Comparison of thermal performances between SMMHP [6] and TMMHP for water

Sl. No.	Parameters	SMMHP [6]	TMMHP	Remarks
1	Thermal conductivity (k)	Constant	Variable	Rate of heat removal is increased in TMMHP.
2	Bandwidth of condensation temperature (Water, 0° incln.)	Small 3.6° C	Large 12° C	Condensation takes place at higher temp. in TMMHP than in SMMHP.
3	Overall temp. difference between two ends of MHP (Water, 0° incln.)	41.2° C	14.9° C	In TMMHP is much smaller, thus enhances cyclic order and rate of heat removal.

4	Temp. gradient at condenser for water	Negative	Positive	Positivity at TMMHP improves capillary action.
5	Time reqd. to complete cycle (Water, 0° incln.)	2 min	< 1 min	Because of thermal vacuum created in TMMHP for variable conductivity and variable pressure gradient.
6	h/h_{eff} (Water, 0°, 6W)	0.95	1.30	Higher TMMHP value because of super heater effect that makes average temp. high.
7	h_{max} (Water, 0° incln.)	0.48 kW/m^2. °C	0.80 kW/m^2. °C	At TMMHP h_{max} is almost *two times* high.
8	h with respect to increasing Q	~uniform	~uniform	At TMMHP mean value of h is higher than SMMHP.

VII. Validation of the Experimental Setup with Known Results

To validate the present experimental setup and results, four experiments are carried out in the IUT Lab with another setup following the test procedures applied to TMMHP. The setup contained a circular SMMHP made with copper which was tested by the experimenters Hossain et al. [18] for ethanol, methanol and acetone, and operated at 30°, 50°, 70° and 90° angles with the heat inputs of 0.61W, 1.56W, 3.67W, and 8.71W. Out of three fluids, ethanol is selected as the working fluid for the validation test. The specifications of the setup are given in Table 3.

Table 3 : Specifications of the experimental setup

Test Parameters	Dimensions (mm)
Outer diameter of the tube, d_o	2.0
Hydraulic diameter of the tube, d_h	1.8
Length of heat pipe, L	150
Length of evaporator section, L_e	50
Length of adiabatic section, L_a	30
Length of condenser section, L_c	70
Inclinations	30°, 50°, 70°, 90° (vertical)

The values of overall heat transfer coefficient, *U*, obtained from the source [18] are compared with those found from the validation experiment, which are within the proximity of 93% of TMMHP. Similarly, the thermal resistances, *R*, are also compared and found to be within 95% of the known values.

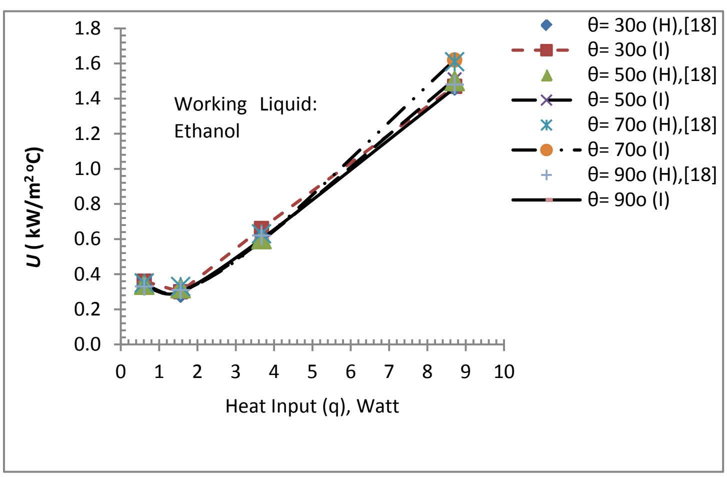

Figure 23 : Validation experiment with the known results [18]

The variation of overall heat transfer coefficient, *U*, at different inclinations are shown in the Fig. 23. In the legendry of the plots, H represents Hossain et al [18] and I for Iqbal (author).

VIII. Uncertainty Analyses

A detailed analysis regarding the uncertainties within the equipment, measurements and results is carried out, which cumulatively is 8.90% with 95% confidence level, According to Kline and McClintock

[19] the total uncertainty propagation for $r = f(v_{j=1...n})$ is summarized in *eqn. 1* which is commonly used in calculating the related uncertainties in any experiment.

$$u(r) = \sqrt{\sum_{j=1}^{n}[\frac{\partial r}{\partial v_j}u(v_j)]^2} \qquad (1)$$

Here, *u* stands for the standard uncertainty, which is equivalent to the standard deviation, and v_j stands for the variables that contribute to the uncertainty in the result *r* that revolves around any data reduction equation. Thus finally, the relative uncertainties for *h* can be cumulatively expressed as in *eqn. 2*

$$\left(\frac{U_h}{h}\right)^2 = \left\{\left(\frac{U_{he}}{h_e}\right)^2 + \left(\frac{U_{ha}}{h_a}\right)^2 + \left(\frac{U_{hc}}{h_c}\right)^2\right\} \times 100\% \qquad (2)$$

or, it can be re-written for standard uncertainty in the form of *eqn. 1* as shown in *eqn. 3*.

$$u(h) = \left\{\sqrt{\sum_{j=e}^{c}\frac{\partial h}{\partial q_j}h(q_j) + \sum_{j=e}^{c}\frac{\partial h}{\partial T_j}h(T_j) + \sum_{j=e}^{c}\frac{\partial h}{\partial A_j}h(A_j)}\right\} \times 100\% \qquad (3)$$

where *j* = *e, a* and *c* which represents evaporator, adiabatic and condenser respectively.

IX. Correlation

A dimensionless correlation has been developed which correlates all the data collected in this study. It is mentioned earlier and shown in the graphs that a few common relations are found between heat transfer coefficient and other operating parameters. These common relations may be shown mathematically as $h = f(\rho(p(q)))$

In a dimensionless relation, the above function can be rewritten along with the calculated constants as follows.

$$\frac{h}{h_{eff}} = 0.468\left(\frac{q"_{e,eff}}{q"_{e,s}}\right)^{-0.041}\left(\frac{q"_{c,s}}{q"_{c,eff}}\right)^{0.076}\left(\frac{\Delta P}{\Delta P_{eff}}\right)^{-0.984}\left(\frac{\rho_c}{\rho_e}\right)^{0.081}\left(\frac{d_T}{d_H}\right)^{0.997}\left(\left\{\frac{l}{l_{eff}}\right\}^{sin\theta cos\theta}\right)^{1.366}$$

Graphical representation of all the correlated data is shown in Figure 23, and 98% of them are found to be within ±15% range of the regression line. Using the acquired data, the correlation produces *h* within the ±18% proximity of the experimental value.

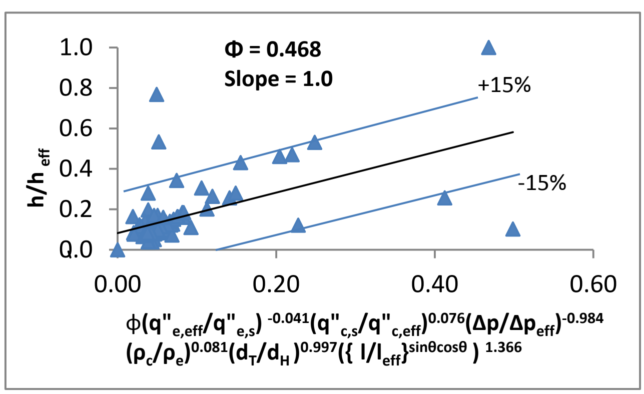

Figure 23 : Graphical representation of the developed correlation of TMMHP

X. Conclusions

From the study, the following conclusions can be drawn.

a) In SMMHP, the terminal temperature difference is very high for water comparing with that produced by TMMHP. As a result, the *h* of the water produced by the TMMHP is much higher than that by SMMHP.

b) Out of four working fluids, *methanol* has been found to provide the highest *h* in all three orientations, because of its low boiling point and density that enables quick completion of thermodynamic cycle.

c) It is proven that MHP made with the metals of variable thermal conductivity, i.e. TMMHP, of ascending order orientation, which initiates the super heater effect in the evaporator, indicates many folds better prospect of *h* value than that of made with constant conductivity, SMMHP [6].

d) While an assumption of single phase flow in SMMHP works well at lower heat inputs, but at moderately high heat inputs it becomes a two-phase flow. However, the super heater effect at the evaporator in TMMHP eliminates that complexity of the two-phase and instantly turns into a single phase flow of vapor which was not possible in SMMHP [6, 7].

e) In case of convergent-divergent TMMHP, the upper trend of temperature at the condenser terminal is uniquely different from that of other geometry. Such a condition demands the coolant flow of lower than the ambient temperature or a coolant of higher C_p. Eventually, this slightly increased temperature of the vapor condensate speeds up the capillary action of the wick.

f) The change of any specific physical property (i.e. density, specific gravity, viscosity) of a fluid singly cannot change the h of that fluid in an MHP, rather it is a compound value developed functionally from both of its physical properties and state variables as of $h = f(\rho(p(q)))$.

g) Since the evaporation-condensation cycle within the convergent-divergent TMMHP takes much small time, which causes the "dry out" situation in the evaporator, an attempt to improve the capillary pumping system within the heat pipe may be undertaken for further research.

h) Since the h values produced by organic and inorganic compounds are found to be characteristically different, non linear and linear respectively, an azetrope (content of mixed fluids at a certain ratio with no chemical reactions) may be used as a working fluid to check the improvement.

NOMENCLATURE

C_p, specific heat at constant pressure, $kJ/kg.^0C$

d_H, hydraulic diameter of the heat pipe, (m)

d_T, profile height of the heat pipe, (m)

h, heat transfer coefficient for terminal temperature difference of the fluid, $kW/m^2.^0C$

h_{eff}, effective heat transfer coefficient for terminal average temperature difference of the fluid, $kW/m^2.^0Cv$

l, length of the heat pipe, m

l_{eff}, effective length of the heat pipe, m

p, pressure of the fluid, $Pa\ (N/m^2)$

q, heat input, *Watt*

Δp, terminal pressure drop, kPa

Δp_{eff}, effective pressure drop at terminal average pressure, kPa

q'', heat flux, kW/m^2

$q''_{e,\,eff}$, effective heat flux through the evaporator shell by conduction, kW/m^2

$q''_{e,\,s}$, heat flux at the evaporator surface supplied by heater, kW/m^2

$q''_{c,\,s}$, dissipated heat flux from the condenser surface by convection cooling, kW/m^2

$q''_{c,\,eff}$, effective heat flux dissipated through the condenser shell by conduction, kW/m^2

R_{eff}, effective thermal resistance, $^oC/Watt$

T_1-T_5, temperatures of the fluids in the micro heat pipe, ^0C

ρ, density of the fluid, kg/m^3

ρ_c, density of the fluid at the condenser, kg/m^3

ρ_e, density of the fluid at the evaporator, kg/m^3

φ, dimensionless correlation constant

θ, angle of inclination, degree (°)

Subscripts:

c, condenser

e, evaporator

eff, effective

p, constant pressure

s, surface of the heat pipe

1-5, positions of thermocouples

XI. Acknowledgement

The experiments are conducted at the Refrigeration and Air-conditioning lab of the Islamic University of Technology (IUT), OIC, Bangladesh. The authors gratefully acknowledge the total financial along with other necessary supports provided by the university in performing this research for Ph.D. program.

References Références Referencias

1. G. P. Peterson, "An Introduction to Heat Pipes-Modeling, testing and applications", John Wiley & Sons, Inc., 1994.
2. G. M. Grover, T. P. Cotter and G. F. Erickson, "Structures of Very High Thermal Conductance", Journal of Applied Physics, 35(6): 1990-1991, 1964.
3. P. D. Dunn and D. A. Reay, "Heat pipes", 3rd Edition, Publisher: Robert Maxwell, Chapter 1-5, 1982.
4. T. N. Sreenivasa, S. N. Sridhara and G. Pundarika, "Working fluid inventory in miniature heat pipe", Proceedings of the International Conference on Mechanical Engineering (ICME'05), Dhaka, Bangladesh, 2005.
5. M. A. R. Akhanda, S. L. Mahmood and Ashik Ahmed, "An experimental investigation of an air-cooled miniature heat pipe (MHP) using different working fluids at different fill ratios", Proceedings of the 3rd BSME-ASME International Conference on Thermal Engineering, Dhaka, Bangladesh, Paper No. BA 175, 2006.
6. S. L. Mahmood, "Experimental Investigation on Micro Heat Pipes of Different Cross-sections having same Hydraulic Diameter", MS Thesis, Islamic University of Technology, OIC, Bangladesh, September 2007.
7. A. S. Annamalai and V. Ramalingam, "Experimental investigation and computational fluid dynamics analysis of an air cooled condenser heat pipe", THERMAL SCIENCE, 15(3): 759-772, 2011.
8. KMN S. Iqbal, "Thermal performances of two-metal (Cu-Ag) micro heat pipe (TMMHP)", Ph.D. Thesis, Islamic University of Technology, OIC, Bangladesh, November, 2014.
9. *S. H. Moon,* "Improving Thermal Performance of Miniature Heat Pipe for Notebook PC Cooling", pages: 135-140, January 2002.
10. B. R. Babin, G. P. Peterson, and D.Wu, "Steady-state Modeling and Testing of a Micro Heat Pipe," *J. Heat Transfer*, Vol. 112*,* 595-601,1990.
11. S. W. Chi, "Heat Pipe Theory and Practice," McGraw-Hill, NY, U.S.A., 1976.
12. J. Longtin, B. F. Badran, and M. Gerner, "A One-dimensional Model of a Micro Heat Pipe during Steady-state Operation," J. Heat Transfer, Vol. 116, 709-715, 1994.
13. L. W. Swanson and G. P. Peterson, "The Interfacial Thermodynamics of the Capillary Structures in Micro Heat Pipes," J. Heat Transfer, Vol.17, pp. 195-201,1995.
14. D. Wu and G. P., Peterson, "Investigation of the Transient Characteristics of a Micro Heat Pipe," J. Thermo physics, Vol. 5,129-134, 1991.
15. M. Le Berre, G. Pandraud, P. Morfouli, and M. Lallemand," The performance of micro heat pipes measured by integrated sensors". Journal of Micromechanics and Microengineering, 16:1047–1050, 2006.
16. Madhusree Kole and Dev, "Thermal performance of screen mesh wick heat pipes using water based copper nanofluids", last visited on June 02, 2014.
17. *Yuan-Ching Chiang, Jen-Jie Chieh* and *Chia-Che Ho,* "The magnetic-nano fluid heat pipe with superior thermal properties through magnetic enhancement", last visited on June 02, 2014.
18. *Hossain, R.A.,* Chowdhuri, M.A.K, Feroz, C. M., "Design, Fabrication and Experimental Study of Heat Transfer Characteristics of a Micro Heat Pipe", Jordan Journal of Mechanical and Industrial Engineering, Volume 4, Number 5, Pages 531- 542, 2010.
19. Kline, S. J. and McClintock, F. A., "Describing the uncertainties in single sample experiments". Mechanical Engineering, pages 3–8, 1953.